

**Sources, fluxes, and behaviors of fluorescent dissolved organic matter (FDOM) in the
Nakdong-River Estuary, Korea**

Shin-Ah Lee¹ and Guebuem Kim^{1*}

¹School of Earth and Environmental Sciences/Research Institute of Oceanography, Seoul
National University, Seoul 08826, Republic of Korea

*Corresponding author. Tel : +82-2-880-7508; Fax : +82-2-876-6508

E-mail address: gkim@snu.ac.kr (G.Kim)

Submitted to *Biogeosciences* (Revised version)

Abstract

We monitored seasonal variations of dissolved organic carbon (DOC), stable carbon isotope of DOC ($\delta^{13}\text{C}$ -DOC), and fluorescent dissolved organic matter (FDOM) in water samples from a fixed station in the Nakdong-River Estuary, Korea. Sampling was performed every hour during spring tide once a month from October 2014 to August 2015. The concentrations of DOC and humic-like FDOM showed significant negative correlations against salinity ($r^2=0.42-0.98$, $p < 0.0001$), indicating that the river-originated DOM components are the major source and behave conservatively in the estuarine mixing zone. The extrapolated $\delta^{13}\text{C}$ -DOC values ($-27.5 - 24.5\text{‰}$) in fresh water confirm that both components are mainly of terrestrial origin. The slopes of humic-like FDOM against salinity were 60-80% higher in the summer and fall, due to higher terrestrial production of humic-like FDOM. The slopes of protein-like FDOM against salinity, however, were 70-80% higher in spring, due to higher biological production in river water. Our results suggest that there are large seasonal changes in riverine fluxes of humic and protein-like FDOM to the ocean.

1. Introduction

The global annual flux of dissolved organic carbon (DOC) via rivers is approximately $0.17 - 0.36 \times 10^{15}$ g (Meybeck, 1982; Ludwig et al., 1996; Dai et al., 2012). The DOC delivered from riverine discharges as well as *in situ* production through biological activities significantly affects carbon and biogeochemical cycles in coastal waters (Hedges, 1992; Bianchi et al., 2004; Bauer et al., 2013; Moyer et al., 2015).

Generally, DOC includes fluorescent dissolved organic matter (FDOM), which emits fluorescent light due to its chemical characteristics. As FDOM accounts for 20 - 70% of the DOC in coastal waters (Coble, 2007) and controls the penetration of harmful UV radiation in the euphotic zone, it plays a critical role in carbon cycles as well as biological production. In addition, FDOM is known as a powerful indicator of humic and protein-like substances (Coble, 2007) in coastal waters. River discharge is generally the main source of humic-like FDOM in coastal waters, although it is also produced through *in situ* microbial activity (Romera-Castillo et al., 2011). In contrast, protein-like FDOM is known to be from biological production as well as anthropogenic sources (Baker and Spencer, 2004). Terrestrial humic substances behave conservatively in coastal areas due to their refractory characteristics (Del Castillo et al., 2000), whereas protein substances behave non-conservatively in many estuaries due to their relatively rapid production and degradation (Vignudelli et al., 2004).

The magnitudes of DOC and FDOM fluxes from rivers are generally dependent on rainfall, discharge, and temperatures (Maie et al., 2006; Jaffé et al., 2004; Huang and Chen,

2009). In the estuarine mixing zone, intensive biogeochemical processes occur through photo-oxidation, microbial degradation, or physicochemical transformations (i.e., flocculation, sedimentation) (Bauer and Bianchi, 2011; Moran et al., 1991; Benner and Opsahl, 2001; Raymond and Bauer, 2001). Recent studies have demonstrated large seasonal variations as high as 40%, in DOC export from rivers to the ocean (Burns et al., 2008; Bianchi et al., 2004; Dai et al., 2012). However, the seasonal variations in sources, fluxes, and behaviors of DOC and FDOM in the estuarine mixing zone are still poorly understood.

In this study, we analyzed DOC, $\delta^{13}\text{C}$ -DOC, and FDOM in estuarine water samples collected monthly from the Nakdong-River estuary. Sampling was conducted at a fixed platform, which has been utilized for monitoring various environmental parameters. This sampling station is advantageous because we can collect water samples for a wide range of salinities throughout tidal fluctuations. Using the data obtained from this unique station, we were able to determine (1) the behaviors of DOM in the estuarine mixing zone, (2) the fluxes of DOM from rivers based on the slopes between salinities and DOM components, and (3) the changes in DOM sources using $\delta^{13}\text{C}$ -DOC in the estuarine samples. The slope measurement in the mixing zone may represent the endmember of DOM components in rivers better than site-specific measurements in the river, by integrating larger spaces and times.

2. Materials and methods

2.1 Study site

The Nakdong-River Estuary, which is the estuary of the longest river in Korea, is a

major source of water supplying the needs for drinking, agriculture, and industry. The main channel of Nakdong River is approximately 510 km in length with a watershed area of approximately 23,380 km². It faces the south-eastern coastal area of the Korean peninsula, passing through Busan which is the second largest city in Korea. The mean annual precipitation is 1150 mm, and most precipitation (60-70%) occurs during the summer monsoon and typhoon seasons (Jeong et al., 2007). To manage water supply and saltwater intrusion, estuary dams were constructed in the mouth of the river in 1987.

2.2 Sampling

Water samples were collected at the sampling site which is located 560 m downstream from the dam (Fig. 1). The sampling period was from October 2014 to August 2015. The 2-L water sampling was conducted every hour for 24 hours during spring tide using an auto-sampler (RoboChemTMAutosampler, Model S3-1224N, Centennial Technology, Korea), with a depth of the water intake 1 m below the surface. After samples were collected in acid-cleaned polyethylene bottles, they were moved to the laboratory within 24 hours. All water samples were filtered using pre-combusted GF/F filters. The FDOM samples were stored in pre-combusted amber glass vials and kept below 4°C in a refrigerator before analysis. The DOC and $\delta^{13}\text{C}$ -DOC samples were acidified to pH ~2 using 6 M HCl to avoid bacterial activities and stored in pre-combusted glass ampoules. Ampoules were fire-sealed to prevent the samples from any contaminations. The samples were analyzed for DOC and CDOM within a week. Salinity was measured using a YSI Pro Series conductivity probe sensor in the laboratory. The real-time and compulsory discharge volume data from the dam are available at <http://www.water.or.kr>, provided by K-Water. The monitoring program at this station is

maintained by Korea Environment Management Corporation (KOEM). The water temperature data are recorded automatically at the site. The data are available at <https://www.koem.or.kr>.

2.3 Analytical methods

The concentrations of DOC were determined by a high-temperature catalytic oxidation (HTCO) method using a TOC-VCPH analyzer (Shimadzu, Japan). Standardization was performed based on the calibration curve of acetanilide in ultra-pure water. The acidified samples were purged with carbon dioxide (CO₂) free carrier gas for 2 min to remove inorganic carbon. The samples were then injected into a combustion column packed with Pt-coated alumina beads and heated to 720°C. The CO₂ evolving from combusted organic carbon was detected by a non-dispersive infrared detector (NDIR). Our DOC method was verified with Deep Seawater Reference (DSR) samples for DOC (44-46 µmol L⁻¹) produced by the University of Miami, USA.

The values of δ¹³C-DOC were measured using a TOC-IR-MS instrument consisting of an IR-MS instrument coupled with a Vario TOC cube (Isoprime, Elementar, Germany). The TOC instrument uses a common high-temperature catalytic combustion method (Kirkels et al., 2014). The analytical method is fully described in Kim et al. (2015). Briefly, 10 mL of filtered samples was purged with O₂ gas for 20–30 min to completely remove DIC after the samples were acidified to pH ~2. Then, 1 mL of the sample was injected into Pt-impregnated catalyst in a quartz tube. In this tube, the DOC was converted completely to CO₂ at 750°C, which was then fed through a water trap followed by a halogen trap. After DOC was detected by an NDIR

detector, the CO₂ gas was entered the TOC–IR–MS interface by the O₂ carrier gas. In the interface, the CO₂ was transferred to the IR–MS instrument following the removal of any interfering gasses. The $\delta^{13}\text{C}$ -DOC value of blank was measured using the Low Carbon Water (LCW) from Hansell lab (University of Miami), which contains less than 2 μM DOC. Certified IAEA-CH6 sucrose (International Atomic Energy Agency, $-10.45 \pm 0.03\text{‰}$) prepared with the low carbon water was used as a standard solution. A standard sample was analyzed for every sample queue (once before or after ten samples) to check a drifting effect during the measurements. The blank correction was performed using a method previously described in De Troyer et al. (2010) and Panetta et al. (2008). Our measurement result of $\delta^{13}\text{C}$ -DOC for the DSR (University of Miami) was $-21.5 \pm 0.1\text{‰}$, which is consistent with the results reported by Panetta et al. (2008) and Lang et al. (2007). The reproducibility of TOC–IR–MS was $\sim 0.3\text{‰}$.

FDOM fluorescence was determined in a scan mode using a spectrofluorometer (SCINCO FluoroMate FS-2) within two days after sampling. Emission (Em) spectra were collected from 250 to 600 nm at 2 nm intervals at excitation (Ex) wavelengths from 250 nm to 500 nm at 5 nm intervals. Backgrounds were subtracted for fresh distilled water prepared daily from the sample data to eliminate Raman Scatter peaks (Zepp et al., 2004). All data were obtained in counts per second (cps) and converted to a ppb quinine sulfate standard solution in 0.1 N sulfuric acid at Ex/Em of 350/450 nm. The inner filter effect was negligible for these estuarine water samples since the correlation between the uncorrected and corrected values for the inner filter effect was very significant for the three identified peaks ($r^2=1$, $n=5$). EEMs-PARAFAC analysis was performed using a MATLAB R2013a program with a DOMFluor toolbox.

3. Results and Discussion

Salinities ranged from 0.1 to 28.5 over the sampling period of a year. Salinities in the sampling location were dependent primarily on the volume of river-water discharge from the dam. The volumes of river discharge were relatively larger in October, April, July, and May. The mean annual surface water temperature was 16°C, with the lowest temperature (avg. 8°C) in December and the highest temperature in August (avg. 26°C).

3.1 Behaviors and sources of DOC in the estuarine mixing zone

The concentrations of DOC ranged from 100 to 300 µM, with the highest concentrations in July (avg. 243 µM) and the lowest concentrations in February (avg. 115 µM), consistent with the typical DOC concentration ranges in coastal waters (Wang et al., 2004; Raymond and Bauer, 2001). The concentrations of DOC correlated significantly with salinities ($r^2 = 0.59-0.92$, $p < 0.0001$), indicating that DOC behaves conservatively in the mixing zone of this estuary (Fig. 2A), which is commonly observed in estuarine mixing zones (Laane, 1980; Mantoura and Woodward, 1983; Del Castillo et al., 2000; Clark et al., 2002; Jaffé et al., 2004).

If the high salinity periods are excluded, both the slope and y-intercept of DOC concentrations versus salinities were highest in July (Fig. 2), which could be due to a higher terrestrial DOC loading in the summer period, as observed in Horsens Fjord, Denmark (Markager et al., 2011). For this comparison, we excluded the high-salinity periods (>20), including December, January, February, and June, since they showed a narrow and low DOC

concentration range (103-163 μM), resulting in large uncertainties by extrapolating them to the fresh water.

The carbon isotope values in the Nakdong-River Estuary ranged from -28.2 ‰ to -17.6. In order to determine the source of DOC in fresh water, we plotted $\delta^{13}\text{C}$ -DOC values against salinities (Fig. 2B). The conservative mixing curve of $\delta^{13}\text{C}$ values can be obtained using the two endmember mixing equation (Spiker, 1980; Raymond and Bauer, 2001):

$$\delta^{13}\text{C}_s = \frac{F_r \delta^{13}\text{C}_r [\text{DOC}]_r + (1-F_r) \delta^{13}\text{C}_m [\text{DOC}]_m}{[\text{DOC}]_s} \quad (1)$$

where $\delta^{13}\text{C}_s$, $\delta^{13}\text{C}_r$ and $\delta^{13}\text{C}_m$ are the $\delta^{13}\text{C}$ -DOC values at a given sample salinity, river endmember salinity, and marine endmember salinity, respectively; F_r is the riverine freshwater fraction calculated from the measured salinities; $[\text{DOC}]_s$ and $[\text{DOC}]_m$ are the DOC concentrations at a given salinity and marine endmember salinity, respectively; $[\text{DOC}]_r$ is the endmember DOC value for the river water (Fig. 2).

The riverine DOC endmember values ($S=0\text{‰}$) ranged from 174 to 284 μM . The marine endmember value ($S=29\text{‰}$) of DOC is 100 μM with the $\delta^{13}\text{C}$ -DOC value of -19‰. If these values from each month are applied, the $\delta^{13}\text{C}$ -DOC endmember values for the river water extrapolated to be from -27.5 to -24.5‰ (average: -26.2‰). Overall, the carbon isotope values of our samples are fitted well into the conservative mixing curve of the overall trend, with a slight change using different endmember values for different months (Fig. 2B). In general, $\delta^{13}\text{C}$ -DOC values range from -22 to -18‰ for marine phytoplankton, from -34‰ to -23‰ for terrestrial C3 plants, and from -16‰ to -10‰ for terrestrial C4 plants (Gearing 1988; Clark

and Fritz, 1997). Carbon isotope values in our study confirm that the main source of DOC in the estuarine mixing zone is dominantly from terrestrial C3 plants over all seasons. However, the value was heavier at lower salinity ranges ($S < 10$) in March and April samples, perhaps in association with the higher biological production in the river.

3.2 Behaviors and sources of FDOM in the estuarine mixing zone

Three components were identified in the water samples from the EEMs dataset. Based on the excitation-emission peak location, Component 1 (FDOM_H, Ex/Em = 320/418 nm) is found to be a terrestrial humic-like component (C peak) shown by Coble (2007). Component 2 (FDOM_P, Ex/Em = 280/328 nm) is found to be a tryptophan-like component (T peak), which is produced by microbial processes. Component 3 (Ex/Em = 300,325/364 nm) is found to be a marine humic-like component (M peak). Since Component 3 values were significantly correlated with Component 1 ($r^2=0.95$) values, we simply focused on Component 1 (FDOM_H) and Component 2 (FDOM_P) for data interpretations.

The concentrations of FDOM_H ranged from 2.4 to 19.7 quinine sulfate unit (QSU), with the highest concentration in July (avg. 17.6 QSU) and the lowest concentration in June (avg. 3.4 QSU) (Fig. 2C). The concentrations of FDOM_P ranged from 0.6 to 22.4 QSU, with the highest concentration in March (avg. 15.1 QSU) followed by October (avg. 13.6 QSU) (Fig. 2D).

The concentrations of both FDOM components were significantly correlated with salinities ($r^2 = 0.42-0.98$, $p < 0.0001$ for FDOM_H and $r^2 = 0.27-0.96$, $p < 0.0001$ for FDOM_P), indicating that they are conservative in the mixing zone (Fig. 2). The slopes of FDOM_H and FDOM_P for each month ranged from -0.15 to -0.59 and -0.15 to -0.71, respectively. The higher FDOM_H slopes in July and October were similar to the trend of DOC (Fig. 2C), which could be due to higher terrestrial FDOM production. However, the seasons (March and April) in which higher FDOM_P slopes occurred differ from those of DOC and FDOM_H, indicating that both FDOM components have different source inputs (Fig. 2D).

Although there are large differences in scattering of FDOM components against salinities, it is very difficult to compare scatterings for different seasons in order to discuss the different behaviors of DOM since the scattering is generally larger for the narrow salinity ranges. If the winter data are excluded, in March, during the highest biological production period in the river, the correlation coefficient against salinities was the highest for FDOM_P and lowest for FDOM_H. In contrast, in June, during the highest fluvial DOM discharge period, the correlation coefficient against salinities was the highest for FDOM_H and lowest for FDOM_P. This suggests that the biological production and removal, together with other generally known factors such as photo-degradation and sedimentary inputs, may affect the scattering of these FDOM components in the estuarine mixing zone.

As such, there was a significant positive correlation between FDOM_H and DOC concentrations throughout all sampling periods ($r^2 = 0.93$, $p < 0.0001$) (Fig. 3A), suggesting that the main source of FDOM_H and DOC is terrestrial based on $\delta^{13}\text{C}$ -DOC values. Since FDOM

does not usually contribute to a major portion of DOC, a positive correlation between FDOM and DOC has only been observed in specific areas, such as river-estuarine systems (Del Vecchio and Blough, 2004; Coble, 2007). Stedmon et al., (2006) demonstrated that stronger correlations were observed between DOC and FDOM as humic substances derived from terrestrial DOM are more colored than DOM produced *in situ*. In general, terrestrial DOM occurring in rivers originates mainly from plant decomposition and leaf litter in the form of humic substances (Huang and Chen, 2009). As such, Gueguen et al., (2006) showed that humic materials are more effectively leached from soils during August and September under high temperatures. Thus, higher FDOM_H slopes in August, October, and November, relative to the other periods, could be associated with higher terrestrial inputs of degradation products of soil organic matter (Dowell, 1985; Qualls et al., 1991).

In the study region, FDOM_P concentrations were poorly correlated with DOC concentrations ($r^2=0.11$) (Fig. 3B). The slopes of FDOM_P concentrations against DOC concentrations varied significantly over different seasons, with steeper gradients in the spring (March and April) and fall (October). In general, FDOM_P is known to be produced efficiently by biological production in water (Coble, 1996; Belzile et al., 2002; Steinberg et al., 2004; Zhao et al., 2017). Thus, higher FDOM_P concentrations, relative to DOC concentrations, in the spring and fall seems to be associated with the spring and fall phytoplankton blooms in river waters (Mayer et al., 1999; Zhang et al., 2009).

3.3 Fluxes of DOC and FDOM in the estuarine mixing zone

The fluxes of DOC and FDOM from rivers to the ocean are calculated using the endmember values (C) of these components in rivers multiplied by the river discharge volumes (Q) for each month (Fig. 4). For this estimation, we assumed that (1) the endmember values are the same as the intercepts of the DOC, FDOM_H, and FDOM_P versus salinity plots, and (2) the endmember values measured in the spring tides represent the concentrations of these components for each month.

River discharge was highest in April and July following heavy precipitation, and the largest discharge volume was about five-fold higher than that of winter discharges (Fig. 4A). However, the monthly variations of DOC endmember (y-intercept) values were quite constant, ranging from 174 - 284 μM . This indicates that the concentrations of DOC in the river are independent of river discharge volumes (Fig. 4B). The DOC endmember values were highest in December, followed by July and June (Fig. 4B). The monthly variation trend of FDOM_H endmember values was similar to that of DOC, except for the December value. Excluding the December values, the FDOM_P endmember values were highest in March, February, and October. These endmember trends are consistent with the slope variations explained in the previous section. Although there are large uncertainties in fresh water endmember values of DOC and FDOM in winter owing to narrow, high salinity ranges, we used the endmember values for the flux comparisons since the contribution of the uncertainties may be relatively small due to smaller river discharge volumes in winter.

The riverine DOC flux ranged from $1.6 \times 10^6 \text{ mol day}^{-1}$ (February) to $12.3 \times 10^6 \text{ mol day}^{-1}$ (July), indicating that there are large variations of DOC fluxes to the ocean. The riverine

flux of FDOM_H and FDOM_P ranged from 1.4×10^9 QSU m³ day⁻¹ (December) to 23.1×10^9 QSU m³ day⁻¹ (July) and from 1.6×10^9 QSU m³ day⁻¹ (June) to 16.4×10^9 QSU m³ day⁻¹ (March), respectively. The seasonal variation trend of FDOM_H was similar to that of DOC. The fluxes of FDOM_P in December and March were twofold higher than those of FDOM_H whereas the flux of FDOM_H in July was 2-3 folds higher than that of FDOM_P. This shows that the fluxes of both components of FDOM differ significantly by seasons owing to the different source inputs even though their magnitudes are controlled mainly by river discharges

It is well known that the single sampling event is not enough to capture the full range of natural variability in DOM abundance over all seasons (Stedmon et al., 2006; Huang and Chen, 2009; Markager et al., 2011; Dai et al., 2012; Moyer et al., 2015). Overall, our results show that monthly variations are significant. This implies that our understanding of DOC fluxes from large rivers is largely biased, depending on sampling resolution, methods, and hydrogeological settings of a specific river. For example, if summer data are extrapolated to annual river water discharge, the DOC and FDOM_H fluxes can be overestimated up to three times for the Nakdong River.

4. Conclusions

The concentrations of FDOM_H and DOC showed significant negative correlations against salinities throughout all sampling periods, indicating that they behave conservatively in this estuarine mixing zone. The slopes of both DOC and FDOM_H concentrations versus salinities were highest in July, due to the largest terrestrial DOC loadings. The carbon isotope values showed that the main source of DOC in the estuarine mixing zone is terrestrial C₃ plants

over all seasons. The slopes of FDOM_P versus salinity were relatively higher in March and April in association with the spring phytoplankton blooms in river and estuarine waters. The monthly fluxes of DOC, FDOM_H, and FDOM_P showed large seasonal variations (5-10 folds), suggesting that the estimation of annual riverine fluxes of DOC, FDOM_H, and FDOM_P requires careful considerations of seasonal changes in rivers.

Competing interests

The authors declare that they have no conflict of interest.

Acknowledgements

We thank the Korea Marine Environment Management Corporation (KOEM) members for their assistance with sampling and laboratory analyses. This work was supported by the National Research Foundation of Korea (NRF) grant funded by the Korean government (MEST) (NRF-2015R1A2A1A10054309).

References

- Baker, A., and Spencer, R. G.: Characterization of dissolved organic matter from source to sea using fluorescence and absorbance spectroscopy, *Sci. Total Environ.*, 333, 217-232, 2004.
- Bauer, J., and Bianchi, T.: 5.02—dissolved organic carbon cycling and transformation, *Treatise on estuarine and coastal science*. Academic Press, Waltham, 7-67, 2011.
- Bauer, J. E., Cai, W.-J., Raymond, P. A., Bianchi, T. S., Hopkinson, C. S., and Regnier, P. A.:

324 The changing carbon cycle of the coastal ocean, *Nature*, 504, 61, 2013.

325 Belzile, C., Gibson, J. A., and Vincent, W. F.: Colored dissolved organic matter and dissolved
 326 organic carbon exclusion from lake ice: Implications for irradiance transmission and carbon
 327 cycling, *Limnol. Oceanogr.*, 47, 1283-1293, 2002.

328 Benner, R., and Opsahl, S.: Molecular indicators of the sources and transformations of
 329 dissolved organic matter in the Mississippi river plume, *Org. Geochem.*, 32, 597-611, 2001.

330 Bianchi, T. S., Filley, T., Dria, K., and Hatcher, P. G.: Temporal variability in sources of
 331 dissolved organic carbon in the lower Mississippi River, *Geochim. Cosmochim. Acta*, 68, 959-
 332 967, 2004.

333 Burns, K. A., Brunskill, G., Brinkman, D., and Zagorskis, I.: Organic carbon and nutrient fluxes
 334 to the coastal zone from the Sepik River outflow, *Cont. Shelf Res.*, 28, 283-301, 2008.

335 Clark, I.J., and Fritz, P.: *Environmental Isotopes in Hydrogeology*, CRC Press/Lewis Publishers,
 336 Boca Raton, 1997.

337 Clark, C. D., Jimenez-Morais, J., Jones, G., Zanardi-Lamardo, E., Moore, C. A., and Zika, R.
 338 G.: A time-resolved fluorescence study of dissolved organic matter in a riverine to marine
 339 transition zone, *Mar. Chem.*, 78, 121-135, 2002.

340 Coble, P. G.: Characterization of marine and terrestrial DOM in seawater using excitation-
 341 emission matrix spectroscopy, *Mar. Chem.*, 51, 325-346, 1996.

342 Coble, P. G.: Marine optical biogeochemistry: the chemistry of ocean color, *Chem. Rev.*, 107,
 343 402-418, 2007.

344 Dai, M., Yin, Z., Meng, F., Liu, Q., and Cai, W.-J.: Spatial distribution of riverine DOC inputs

345 to the ocean: an updated global synthesis, *Curr. Opin. Environ. Sustainability*, 4, 170-178,
 346 <https://doi.org/10.1016/j.cosust.2012.03.003>, 2012.

347 De Troyer, I., Bouillon, S., Barker, S., Perry, C., Coorevits, K., and Merckx, R.: Stable isotope
 348 analysis of dissolved organic carbon in soil solutions using a catalytic combustion total organic
 349 carbon analyzer-isotope ratio mass spectrometer with a cryofocusing interface, *Rapid Commun.*
 350 *Mass Spectrom.*, 24, 365-374, 2010.

351 Del Castillo, C. E., Gilbes, F., Coble, P. G., and Müller-Karger, F. E.: On the dispersal of
 352 riverine colored dissolved organic matter over the West Florida Shelf, *Limnol. Oceanogr.*, 45,
 353 1425-1432, 2000.

354 Del Vecchio, R., and Blough, N. V.: Spatial and seasonal distribution of chromophoric
 355 dissolved organic matter and dissolved organic carbon in the Middle Atlantic Bight, *Mar.*
 356 *Chem.*, 89, 169-187, 2004.

357 Dowell, W. H.: Kinetics and mechanisms of dissolved organic carbon retention in a headwater
 358 stream, *Biogeochemistry*, 1, 329-352, 1985.

359 Gearing, J.N., The use of stable isotope ratios for tracing the nearshore–offshore exchange of
 360 organic matter. In: Jansson, B.-O. (Ed.), *Coastal-Offshore Ecosystem Interactions*, Springer-
 361 Verlag, Berlin, 69–101, 1988.

362 Gueguen, C., Guo, L., Wang, D., Tanaka, N., and Hung, C.-C.: Chemical characteristics and
 363 origin of dissolved organic matter in the Yukon River, *Biogeochemistry*, 77, 139-155, 2006.

364 Hedges, J. I.: Global biogeochemical cycles: progress and problems, *Mar. Chem.*, 39, 67-93,
 365 1992.

366 Huang, W., and Chen, R. F.: Sources and transformations of chromophoric dissolved organic
 367 matter in the Neponset River Watershed, *Journal of Geophysical Research: Biogeosciences*,
 368 114, 2009.

369 Jaffé, R., Boyer, J., Lu, X., Maie, N., Yang, C., Scully, N., and Mock, S.: Source
 370 characterization of dissolved organic matter in a subtropical mangrove-dominated estuary by
 371 fluorescence analysis, *Mar. Chem.*, 84, 195-210, 2004.

372 Jeong, K.-S., Kim, D.-K., and Joo, G.-J.: Delayed influence of dam storage and discharge on
 373 the determination of seasonal proliferations of *Microcystis aeruginosa* and *Stephanodiscus*
 374 *hantzschii* in a regulated river system of the lower Nakdong River (South Korea), *Water Res.*,
 375 41(6), 1269-1279.

376 Kim, T.-H., Kim, G., Lee, S.-A., and Dittmar, T.: Extraordinary slow degradation of dissolved
 377 organic carbon (DOC) in a cold marginal sea, *Sci. Rep.*, 5, 2015.

378 Laane, R.: Conservative behaviour of dissolved organic carbon in the Ems-Dollart estuary and
 379 the western Wadden Sea, *Neth. J. Sea Res.*, 14, 192-199, 1980.

380 Lang, S. Q., Lilley, M. D., and Hedges, J. I.: A method to measure the isotopic (^{13}C)
 381 composition of dissolved organic carbon using a high temperature combustion instrument, *Mar.*
 382 *Chem.*, 103, 318-326, 2007.

383 Ludwig, W., Probst, J. L., and Kempe, S.: Predicting the oceanic input of organic carbon by
 384 continental erosion, *Global Biogeochem. Cycles*, 10, 23-41, 1996.

385 Maie, N., Boyer, J. N., Yang, C., and Jaffé, R.: Spatial, geomorphological, and seasonal
 386 variability of CDOM in estuaries of the Florida Coastal Everglades, *Hydrobiol.*, 569, 135-150,
 387 2006.

388 Mantoura, R., and Woodward, E.: Conservative behaviour of riverine dissolved organic carbon
 389 in the Severn Estuary: chemical and geochemical implications, *Geochim. Cosmochim. Acta*,
 390 47, 1293-1309, 1983.

391 Markager, S., Stedmon, C. A., and S ndergaard, M.: Seasonal dynamics and conservative
 392 mixing of dissolved organic matter in the temperate eutrophic estuary Horsens Fjord, *Estuarine*
 393 *Coastal Shelf Sci.*, 92, 376-388, 2011.

394 Mayer, L. M., Schick, L. L., and Loder, T. C.: Dissolved protein fluorescence in two Maine
 395 estuaries, *Mar. Chem.*, 64, 171-179, 1999.

396 Meybeck, M.: Carbon, nitrogen, and phosphorus transport by world rivers, *Am. J. Sci.*, 282,
 397 401-450, 1982.

398 Moran, M. A., Pomeroy, L. R., Sheppard, E. S., Atkinson, L. P., and Hodson, R. E.: Distribution
 399 of terrestrially derived dissolved organic matter on the southeastern US continental shelf,
 400 *Limnol. Oceanogr.*, 36, 1134-1149, 1991.

401 Moyer, R. P., Powell, C. E., Gordon, D. J., Long, J. S., and Bliss, C. M.: Abundance,
 402 distribution, and fluxes of dissolved organic carbon (DOC) in four small sub-tropical rivers of
 403 the Tampa Bay Estuary (Florida, USA), *Appl. Geochem.*, 63, 550-562, 2015.

404 Panetta, R. J., Ibrahim, M., and G linas, Y.: Coupling a high-temperature catalytic oxidation
 405 total organic carbon analyzer to an isotope ratio mass spectrometer to measure natural-
 406 abundance $\delta^{13}\text{C}$ -dissolved organic carbon in marine and freshwater samples, *Anal. Chem.*, 80,
 407 5232-5239, 2008.

408 Qualls, R. G., Haines, B. L., and Swank, W. T.: Fluxes of dissolved organic nutrients and humic
 409 substances in a deciduous forest, *Ecology*, 72, 254-266, 1991.

410 Raymond, P. A., and Bauer, J. E.: DOC cycling in a temperate estuary: a mass balance approach
 411 using natural ^{14}C and ^{13}C isotopes, *Limnol. Oceanogr.*, 46, 655-667, 2001.

412 Romera-Castillo, C., Sarmiento, H., Álvarez-Salgado, X. A., Gasol, J. M., and Marrasé, C.: Net
 413 production and consumption of fluorescent colored dissolved organic matter by natural
 414 bacterial assemblages growing on marine phytoplankton exudates, *Appl. Environ. Microbiol.*,
 415 77, 7490-7498, 2011.

416 Spiker, E.: The behavior of ^{14}C and ^{13}C in estuarine water: effects of in situ CO_2 production
 417 and atmospheric exchange, *Radiocarbon*, 22, 647-654, 1980.

418 Stedmon, C. A., Markager, S., Søndergaard, M., Vang, T., Laubel, A., Borch, N. H., and
 419 Windelin, A.: Dissolved organic matter (DOM) export to a temperate estuary: seasonal
 420 variations and implications of land use, *Estuaries Coasts*, 29, 388-400, 2006.

421 Steinberg, D. K., Nelson, N. B., Carlson, C. A., and Prusak, A. C.: Production of chromophoric
 422 dissolved organic matter (CDOM) in the open ocean by zooplankton and the colonial
 423 cyanobacterium *Trichodesmium* spp, *Mar. Ecol. Prog. Ser.*, 267, 45-56, 2004.

424 Vignudelli, S., Santinelli, C., Murru, E., Nannicini, L., and Seritti, A.: Distributions of
 425 dissolved organic carbon (DOC) and chromophoric dissolved organic matter (CDOM) in
 426 coastal waters of the northern Tyrrhenian Sea (Italy), *Estuarine Coastal Shelf Sci.*, 60, 133-149,
 427 2004.

428 Wang, X.-C., Chen, R. F., and Gardner, G. B.: Sources and transport of dissolved and
 429 particulate organic carbon in the Mississippi River estuary and adjacent coastal waters of the
 430 northern Gulf of Mexico, *Mar. Chem.*, 89, 241-256, 2004.

431 Zepp, R. G., Sheldon, W. M., and Moran, M. A.: Dissolved organic fluorophores in

432 southeastern US coastal waters: correction method for eliminating Rayleigh and Raman
433 scattering peaks in excitation–emission matrices, *Mar. Chem.*, 89, 15-36, 2004.

434 Zhang, Y., van Dijk, M. A., Liu, M., Zhu, G., and Qin, B.: The contribution of phytoplankton
435 degradation to chromophoric dissolved organic matter (CDOM) in eutrophic shallow lakes:
436 field and experimental evidence, *Water Res.*, 43, 4685-4697, 2009.

437 Zhao, Z., Gonsior, M., Luek, J., Timko, S., Ianiri, H., Hertkorn, N., Schmitt-Kopplin, P., Fang,
438 X., Zeng, Q., and Jiao, N.: Picocyanobacteria and deep-ocean fluorescent dissolved organic
439 matter share similar optical properties, *Nat. Commun.*, 8, 2017.

440

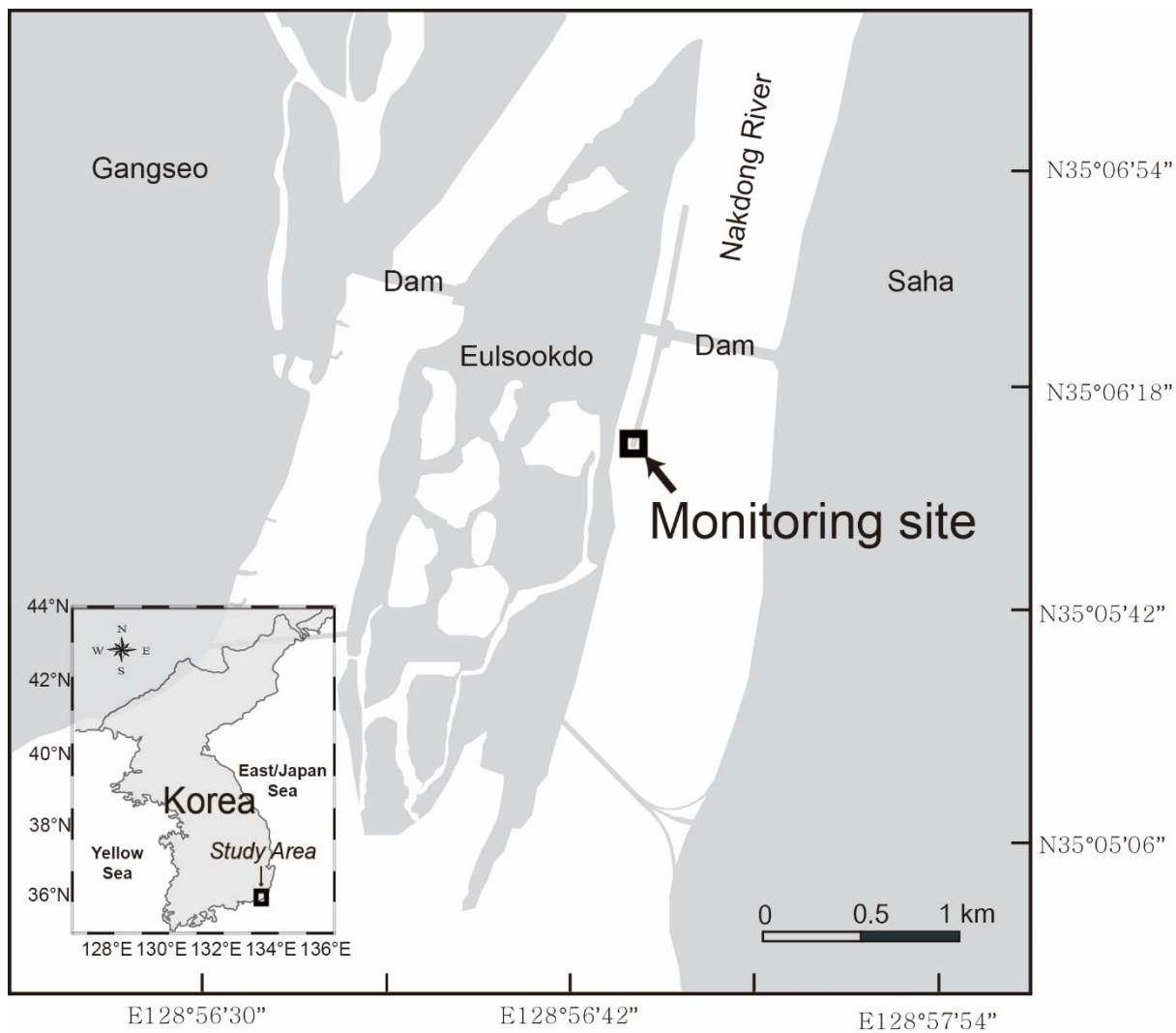


Figure 1. Map of the Nakdong-River Estuary. The square indicates a fixed monitoring site, located 560 m downstream from the dam.

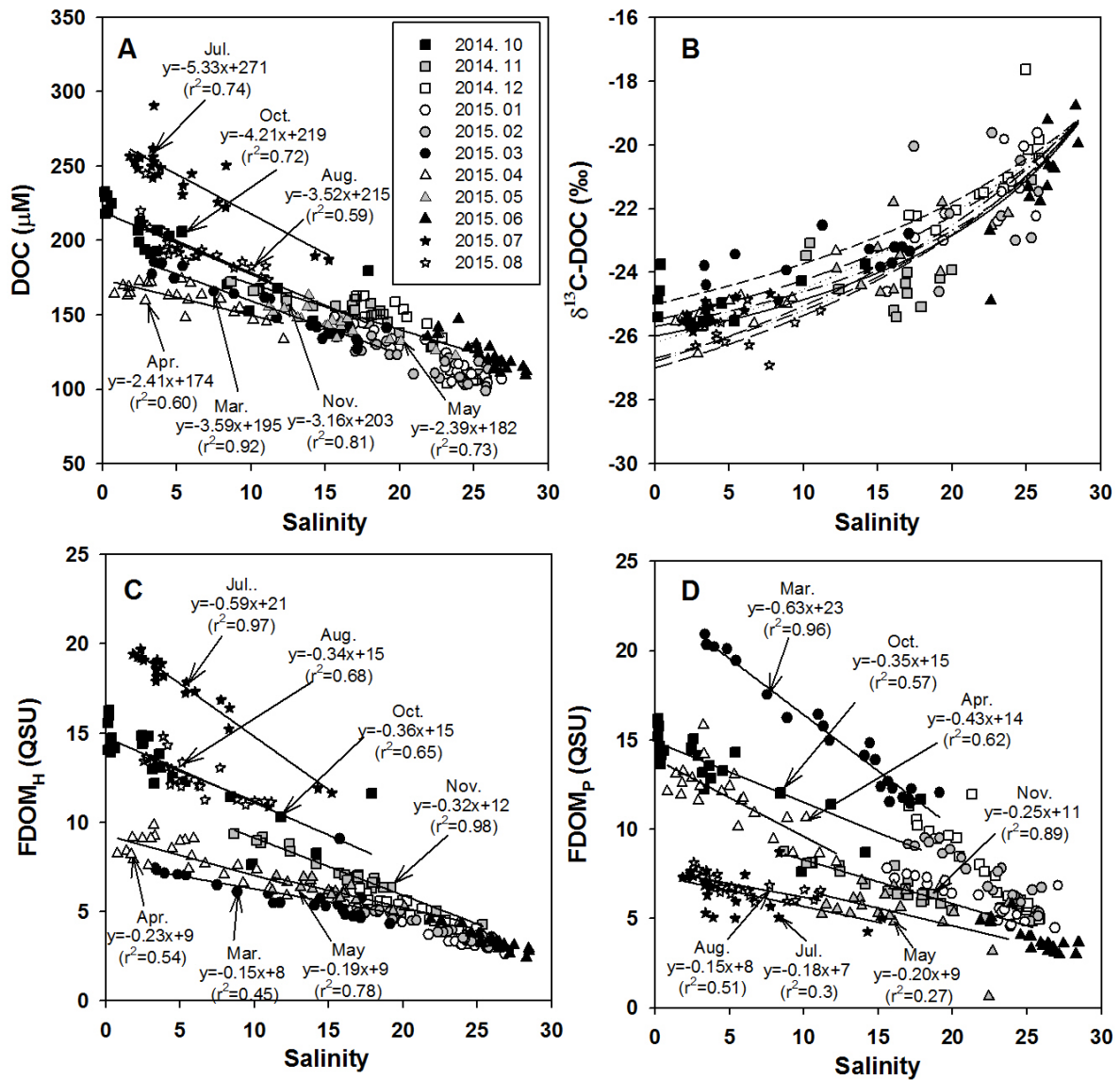


Figure 2. Salinities versus the concentrations of (A) DOC, (B) $\delta^{13}\text{C-DOC}$, (C) FDOM_H, and (D) FDOM_P. The values for the regression lines are excluded for high-salinity periods (>20), including December, January, February, and June, which have large uncertainties in extrapolation. The solid curve (B) is the average conservative mixing line for the two endmember mixing equation. The dotted lines represent the monthly changes in mixing lines for the different monthly endmember values.

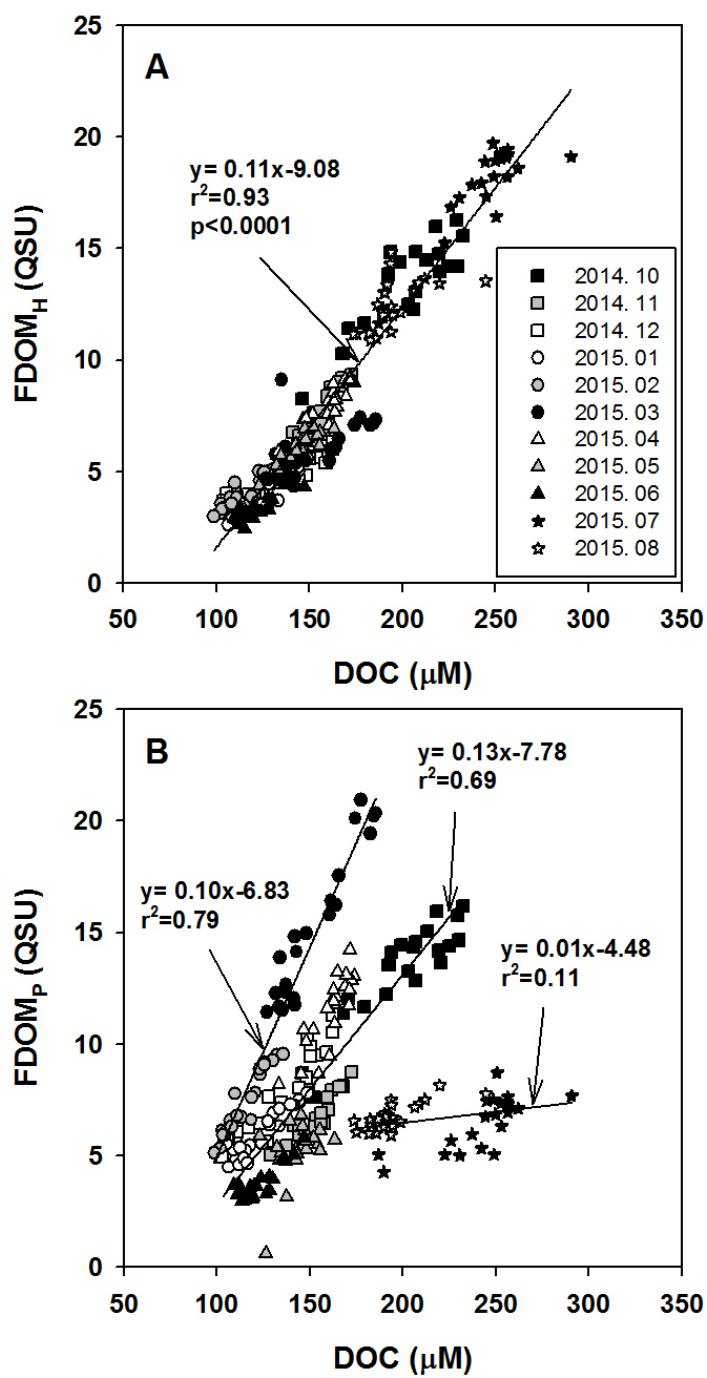


Figure 3. The plots of the concentrations of DOC versus the concentrations of (A) FDOM_H and (B) FDOM_P.

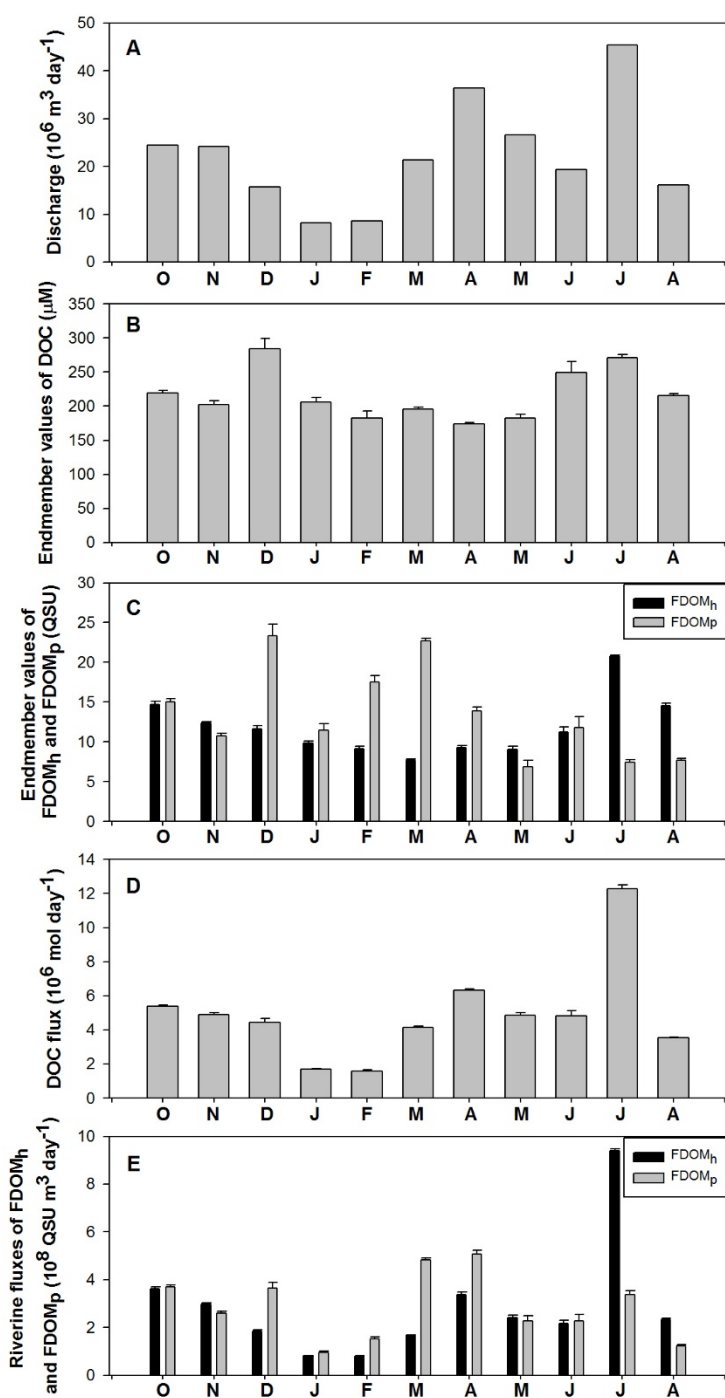


Figure 4. Temporal variations in discharge volumes, the endmember values of DOC, FDOM_H, and FDOM_P, and riverine fluxes of DOC, FDOM_H, and FDOM_P in the Nakdong-River Estuary from October 2014 to August 2015.